PCCP

Local propagating Gaussians: flexible *vs.* frozen widths

Sybil M. Anderson, Tae Jun Park† and Daniel Neuhauser*‡

Department of Chemistry and Biochemistry, University of California, Los Angeles, California 90095-1569, USA. E-mail: dxn@chem.ucla.edu

Received 17th November 1998, Accepted 28th January 1999

Recently we presented a method for modeling a quantum system to a bath that explicitly correlates the system with the individual bath modes. We do this through representation of the bath by locally propagating Gaussians (LPG), which change in position and momentum but remain Gaussian in form. The explicit correlation of the system to the bath modes enters through the simultaneous use of a different Gaussian for each state (or grid point) of the system. In this work, we look at two possibilities for the LPG method. In the frozen LPG, the width of the Gaussians is kept constant. In the flexible LPG, we relax this condition and allow for the width to be both time dependent and complex. We present a comparative study of these two methods and compare them with both time-dependent self-consistent field calculations (TDSCF) and an exact quantum calculation. The two LPG methods, in comparison with TDSCF, more accurately describe the exact dynamics. The difference is especially noticeable in the case of weak coupling, where the averaging done in TDSCF is an oversimplification of the system.

1 Introduction

In spite of the rapid increase in computer speeds in recent years, the exact modeling of a full quantum system remains a daunting task. Full quantum calculations grow exponentially with respect to the number of coupled degrees of freedom; therefore, there has been a continual search for algorithms that give accurate results with minimal computational effort. Consequently, quantum algorithms have developed in two general directions. First, methods for simulating strongly coupled large-amplitude bound and scattered motion for three- and four-body systems have been developed. This is a gargantuan undertaking, because four-body systems require the writing of (at least) six-dimensional wavefunctions.[1–3]

An alternate approach is to look at larger problems, where most of the degrees of freedom are harmonic-like, while only a very few (typically one) degrees of freedom are allowed to be non-harmonic. These type of problems, starting from the well-known spin-boson problem (where a single two-state system is coupled to many harmonic oscillators), have been treated by a host of methods, including path-integral and semi-classical methods,[4–13] matrix-transfer approaches,[14,15] and coupled channel techniques.[16–19] However, the eventual goal (*i.e.*, the treatment of a large system with many anharmonic degrees of freedom, coupled to a large bath) is still exceptionally challenging.

The simplest approach which combines a large bath of oscillators with a system consisting of several degrees of freedom is the time-dependent self-consistent field approximation (TDSCF).[20] In this method, only the expectation values of each degree of freedom are coupled to the other degrees of freedom. TDSCF does not account for the fact that the system and the bath are inter-correlated. For example, if the system is composed of several weakly connected parts, then the bath should, in fact, respond differently to different parts.

A simple approach beyond TDSCF can be derived, as follows. Bath modes are typically only weakly anharmonic; therefore, they can usually be reasonably approximated by a harmonic potential. For a purely harmonic potential, it is well known that an initial Gaussian wavepacket remains Gaussian over time with only its average position, average momentum, and width parameters changing with time. One can postulate that Gaussian behavior should be reasonably accurate even when there is system–bath coupling; however, to take into account the fact that the bath is influenced by the system, and that this influence is different for different system states, we make the following ansatz: *the parameters of the Gaussians that describe the bath are allowed to depend on the system states.* Thus, we end up with an ansatz in which the system and the bath are intrinsically coupled. The approximation is labeled locally-propagating Gaussian (LPG), to emphasize that the bath-Gaussians are propagated differently for different states.

Historically, the advantage of Gaussian wavepackets (GWP) has been well recognized for over the past two decades. Heller originally recognized the advantage of using frozen Gaussian wavepackets on a slowly varying potential.[21] Later, time variational methods were used to propagate these frozen GWP (refs. 22 and 23), and flexible GWP.[24] Out of this initial work there has been a resurgence of interest in GWP.[25–30] Of particular interest here is the use of one frozen GWP per site for coupled electron/nuclear motion.[25] That work, by Diz, Deumens and Ohrn (and the equations used) is analogous to the description here, except for two aspects: the eventual goal, system–bath combinations for a general multi- (and continuous) degree of freedom system; and the use of flexible LPGs, which, in their most complete forms, allow the use of different bath-modes combination for different system sites. On a more general note, the Heisenberg representation was used to propagate frozen GWP.[26] Another method which uses Gaussians is the multiple spawning approach, where an increasing number of frozen-width Gaussians, driven by classical equations, are used as a basis-set for electronic non-adiabatic problems.[29,30] We also mention the suggestion to represent the bath by a product of system-dependent TDSCF modes, rather than Gaussian wavepackets.[15]

The LPG work is fundamentally related to the small-polaron transformation. The small-polaron transformation is an approach to introduce correlation between system and

† On leave from Dongguk University, Seoul 100-715, Korea.
‡ Alfred P. Sloan Fellow, 1996–1998.

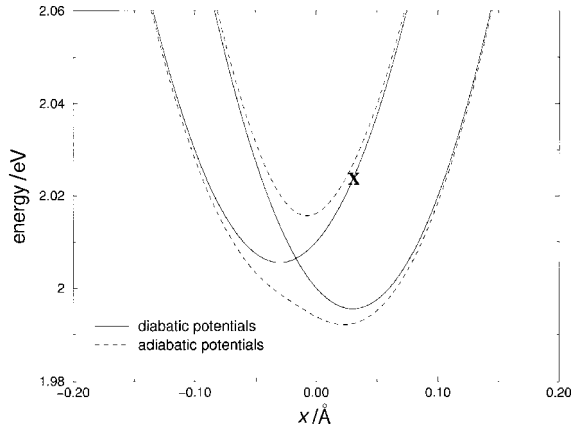

Fig. 1 Potential curves used for testing the LPG studies, on a two-state electron-transfer problem, coupled to a single vibrational-degree of freedom (x). The two solid lines note the diabatic representation, and the dashed lines denote the adiabats. The plots are made for the second and third case in Table 1 (with a slightly lower potential minimum on case II). **X** marks the placement of the initial Gaussian wavepacket, ($\bar{x}$ in the text) for case III.

bath modes through the use of a time-independent correlation factor which shifts the position of the harmonic oscillator for each bath by an amount which is dependent on the system.[31,32] Indeed, in a special case of frozen width, the LPG can be thought of as a time-dependent generalization of the small-polaron transformation.

Although the LPG is easily applied to large-scale calculations, we look here at a simple electron transfer between two valence atoms for our initial comparative studies. This is an example of curve crossing (Fig. 1). (We have encouraging results when looking at a many site proton-transfer system. This will be presented in a later publication.)

In this article, we present both the frozen and flexible LPG, along with a comparison with TDSCF and a full quantum calculation. In Section 2, the TDSCF is reviewed for pedagogical reasons. Then we show the extension to frozen-width LPG. Lastly in this section, we present the new equations for the propagating width. In Section 3, initial results are presented in which the three methods are compared with a full quantum calculation for the simple electron-transfer two site system. In Section 4, we very briefly discuss the ability to model a multi-site system, in which one degree of freedom is exactly done by a quasi-continuous grid and the bath is treated with LPG. Section 5 concludes.

2 Methodology

Throughout the discussion, we consider a system–bath combination with the following Hamiltonian:

$$H = H_{\text{bath}} + H_{\text{system}} + H_{\text{mix}} \tag{1}$$

In these calculations we assume that the bath is a series of N harmonic oscillators. The system is composed of system states denoted by $|i\rangle$. The number of the system states (sites) may vary from 2, as in two-site electron transfer, to a much larger number for a system composed of a quasi-continuous degree of freedom. In this initial calculation, the mixing term that couples the harmonic oscillators and the system is assumed to be a linear. The components of the Hamiltonian are then:

$$H_{\text{bath}} = \frac{\boldsymbol{p}^2}{2m} + \frac{\boldsymbol{x}\cdot\boldsymbol{\kappa}\cdot\boldsymbol{x}}{2} \equiv \sum_n \frac{p_n^2}{2m} + \sum_{ln} \frac{x_n \kappa_{ln} x_l}{2} \tag{2}$$

$$H_{\text{system}} = \sum_{i,j=1}^{\text{sites}} |i\rangle h_{ij} \langle j| \tag{3}$$

$$H_{\text{mix}} = \sum_{i=1}^{\text{sites}} \boldsymbol{\Delta_i}\cdot\boldsymbol{x}\,|i\rangle\langle i| \tag{4}$$

where l and n are the indices for the N bath dimensions; $\boldsymbol{x}$ and $\boldsymbol{p}$ are the bath position and momentum, respectively; m is the oscillators' mass (assumed for simplicity to be bath-mode independent) and $\boldsymbol{\kappa}$ is the force constant tensor. The term h_{ij} is the matrix element of the system Hamiltonian which can include both diagonal and off-diagonal terms. The mixing term ($\boldsymbol{\Delta}_i\cdot\boldsymbol{x} = \Sigma_n \Delta_{in} x_n$) is assumed here to be local so that it does not explicitly couple the different sites $|i\rangle$ and $|j\rangle$, but only each site to the bath (a more general coupling can be assumed). Note that the coupling term makes the overall potential energy surface anharmonic in the bath coordinate.

2.1 TDSCF

For reference, we first examine the TDSCF formalism for the above Hamiltonian. In the TDSCF the effects of the bath and system are separately averaged. The time dependent wavefunction is completely separated into a purely site-dependent component and a purely bath-dependent component. The TDSCF wavefunction is then:

$$\Psi(i, \boldsymbol{x}, t) = \eta(\boldsymbol{x}, t)\psi_i(t) \tag{5}$$

For a harmonic bath, the bath-dependent part $\eta(\boldsymbol{x}, t)$ is a multi-dimensional Gaussian:

$$\eta(\boldsymbol{x}, t) = \frac{(\det \tilde{\boldsymbol{M}})^{1/4}}{\pi^{N/4}} \times \exp\left[-\frac{1}{2}(\boldsymbol{x}-\bar{\boldsymbol{x}})\cdot\tilde{\boldsymbol{M}}\cdot(\boldsymbol{x}-\bar{\boldsymbol{x}}) + i\bar{\boldsymbol{p}}\cdot\boldsymbol{x}\right] \tag{6}$$

where $\bar{\boldsymbol{x}}(t)$ and where $\bar{\boldsymbol{p}}(t)$ are the time-dependent average position and average momentum for the bath. For TDSCF, $\tilde{\boldsymbol{M}}$ is time independent and positive-definite with eigenvalues denoted by $\{1/\sigma_n^2\}_{n=1}^N$.

Given this form of η, the propagation of the wavefunction in terms of $\bar{\boldsymbol{x}}$, $\bar{\boldsymbol{p}}$, and ψ_i is easily derived from the Frenkel variational principle,[33] *i.e.* by minimizing the functional:

$$A = \int_0^\infty \left\langle \Psi \middle| H - i\frac{\partial}{\partial t} \middle| \Psi \right\rangle \mathrm{d}t \tag{7}$$

where $\hbar = 1$. (This same method will also be used to derive the LPG equations of propagation.) Inserting eqn. (5) into eqn. (7), it can easily be shown that:

$$A = \int_0^\infty \mathrm{d}t \left\{ \sum_{j=1}^{\text{sites}} \left[\left(\bar{E} + \bar{\boldsymbol{x}}\cdot\frac{\partial\bar{\boldsymbol{p}}}{\partial t} + \bar{\boldsymbol{x}}\cdot\boldsymbol{\Delta}_j \right) |\psi_j|^2 - i\psi_j^* \frac{\partial\psi_j}{\partial t} \right] + \sum_{j,k=1}^{\text{sites}} \psi_j^* h_{jk} \psi_k \right\} \tag{8}$$

For simplicity, we have defined $\bar{E}$ as the oscillator energy relative to the minimum bath potential. It is calculated as $\bar{E} = \frac{1}{2}(\Sigma_n w_n + \bar{\boldsymbol{x}}\cdot\boldsymbol{\kappa}\cdot\bar{\boldsymbol{x}} + \bar{\boldsymbol{p}}^2/m)$.

All of the equations of motion are found by minimizing the functional A. For $\partial\psi_i/\partial t$, the derivative of A with respect to ψ_i^* is taken and set to zero for each time step. The resulting equation is:

$$\frac{\partial\psi_i}{\partial t} = -i\left\{ \left(\bar{\boldsymbol{x}}\cdot\frac{\partial\bar{\boldsymbol{p}}}{\partial t} + \bar{E} + \bar{\boldsymbol{x}}\cdot\boldsymbol{\Delta}_i \right)\psi_i + \sum_{j=1}^{\text{sites}} h_{ij}\psi_j \right\} \tag{9}$$

The equation for the propagating of the average momentum is found by putting $\partial A/\partial\bar{\boldsymbol{x}} = 0$, resulting in

$$\frac{\partial\bar{\boldsymbol{p}}}{\partial t} = -\left(\bar{\boldsymbol{x}}\cdot\boldsymbol{\kappa} + \bar{\boldsymbol{x}}\cdot\sum_{i=1}^{\text{sites}} \boldsymbol{\Delta}_i \right) \tag{10}$$

To find an expression for the propagation of $\bar{x}$, a canonical transformation is used. Defining

$$\psi_i = \phi_i \mathrm{e}^{-i\bar{x}\cdot\bar{p}} \tag{11}$$

it is straightforward to show that A can be restated as:

$$A = \int \mathrm{d}t \left\{ \sum_{j=1}^{\text{sites}} \left[\left(\bar{E} - \bar{p}\cdot\frac{\partial \bar{x}}{\partial t} + \bar{x}\cdot\Delta_j \right) |\phi_j|^2 - i\phi_j^* \frac{\partial \phi_j}{\partial t} \right] + \sum_{j,k=1}^{\text{sites}} \phi_j^* h_{jk} \phi_k \right\} \tag{12}$$

Notice the $\bar{x}\cdot\partial\bar{p}/\partial t$ has been replaced by a $-\partial\bar{x}/\partial t\cdot\bar{p}$. Differentiation of eqn. (12) with respect to $\bar{p}$ yields:

$$\frac{\partial \bar{x}}{\partial t} = \frac{\bar{p}}{m} \tag{13}$$

The final TDSCF eqns. (9), (10) and (13), are simultaneously propagated. The coupling between the sites is only dependent on the off-diagonal elements of the h_{ij} term.

2.2 Frozen LPG

In the LPG method the TDSCF is extended to have a Gaussian on each site coordinate. The resulting equations are presented here for completeness, and are analogous to those in refs. 25 and 34. We amend the wavefunction to be written as:

$$\Psi(i, \boldsymbol{x}) = \eta_i(\boldsymbol{x}, t)\psi_i(t) \tag{14}$$

where now η_i is a site-dependent Gaussian and has the form:

$$\eta_i(\boldsymbol{x}, t) = \frac{\det(\tilde{\boldsymbol{M}}_i)^{1/4}}{\pi^{N/4}} \times \exp\left[-\frac{1}{2} (\boldsymbol{x} - \bar{x}_i)\cdot\tilde{\boldsymbol{M}}_i\cdot(\boldsymbol{x} - \bar{x}_i) + i\bar{p}_i\cdot\boldsymbol{x} \right] \tag{15}$$

The bath's variables $\bar{x}_i$, $\bar{p}_i$ and $\tilde{\boldsymbol{M}}_i$ are, respectively, the average position, average momentum and the tensor width for the ith Gaussian. (Note the exact meaning of $\bar{x}_i$. It is a vector of N variables, $\bar{x}_{ni}(t)$, where $\bar{x}_{ni}(t)$ refers to the average position of the nth bath degree of freedom for system site i.) In the frozen Gaussian equations for LPG, we take $\tilde{\boldsymbol{M}}_i$ to be time independent and real. These conditions will be removed for the flexible LPG in Section 2.3.

An important distinction of LPG from TDSCF is that the coupling between sites is influenced by the overlap of the individual Gaussians. We define:

$$W_{ij} = \langle \eta_i | \eta_j \rangle = \int_{-\infty}^{\infty} \eta^*(\bar{x}_i, \bar{p}_i, x)\eta(\bar{x}_j, \bar{p}_j, x)\mathrm{d}x \tag{16}$$

The time dependence is in $\bar{x}_i(t)$ and $\bar{p}_j(t)$. Inserting in the form of η from eqn. (15) into eqn. (16), completing the square in the exponential and integrating, the following form for the overlap W_{ij} as follows:

$$W_{ij} = \exp\left\{ -\frac{1}{4\sigma^2} \left[(\bar{x}_i - \bar{x}_j)^2 + \sigma^4(\bar{p}_i - \bar{p}_j)^2 + 2i\sigma^2(\bar{x}_i + \bar{x}_j)\cdot(\bar{p}_i - \bar{p}_j) \right] \right\} \tag{17}$$

This will be used in the derivation of the equations of motion.

Substituting eqns. (14) and (15) for the wavefunction into eqn. (7), the functional A is now written as:

$$A = \int \mathrm{d}t \left\{ \sum_{j=1}^{\text{sites}} \left[\left(\bar{E}_j + \bar{x}\cdot\Delta_j + \bar{x}_j\cdot\frac{\partial \bar{p}_j}{\partial t} \right) |\psi_j|^2 - i\psi_j^* \frac{\partial \psi_j}{\partial t} \right] + \sum_{j,k=1}^{\text{sites}} \psi_j^* h_{jk} \psi_k W_{jk} \right\} \tag{18}$$

Notice that now the coupling between sites depends not only on h_{jk} but also on the Gaussian overlap W_{jk}, as expected.

Once again we minimize A to get equation of motion for the variables. First taking the derivative with respect to ψ_i^*, we very simply get:

$$\frac{\partial \psi_i}{\partial t} = -i \left[\left(\bar{x}_i\cdot\frac{\partial \bar{p}_i}{\partial t} + \bar{E}_i + \bar{x}_i\cdot\Delta_i \right)\psi_i + \sum_{j=1}^{\text{sites}} W_{ij} h_{ij} \psi_j \right] \tag{19}$$

Here, $\bar{E}_i$ is the sum of the oscillators energies relative to the minimum for the ith site and is likewise calculated to be $\frac{1}{2}(\Sigma_n w_n + \bar{x}_i\cdot\kappa\cdot\bar{x}_i + \bar{p}_i^2/m)$.

Similarly, we take the derivative of A with respect to $\bar{x}_i$. Using the definition of the Gaussians and some simple algebra, it follows that:

$$\frac{\partial \bar{p}_i}{\partial t} = -\left\{ \bar{x}_i\cdot\kappa + \Delta_i + \mathrm{Re}\left[\frac{1}{\psi_i} \sum_{j=1}^{\text{sites}} h_{ij}\psi_j W_{ij} \times \left[\frac{1}{\sigma^2}(\bar{x}_j - \bar{x}_i) + i(\bar{p}_j - \bar{p}_i) \right] \right] \right\} \tag{20}$$

As was done for the TDSCF case, we take the canonical transform to get an equation for the time dependence of $\bar{x}_i$, leading to:

$$\frac{\partial \bar{x}_i}{\partial t} = \frac{\bar{p}_i}{m} + \mathrm{Re}\left[\frac{1}{\psi_i} \sum_{j=1}^{\text{sites}} h_{ij}\psi_j W_{ij}[\sigma^2(\bar{p}_j - \bar{p}_i) - i(\bar{x}_j - \bar{x}_i)] \right] \tag{21}$$

In eqns. (20) and (21) the last term (the summation) is new (different from TDSCF), for it explicitly accounts for the coupling between sites.

Because the number of real variables is just $2 + 2N$ per system site, the LPG eqns. (19), (20) and (21) are efficient to solve. Note that the off-diagonal terms in eqn. (19) are dependent on the overlap and determine the coupling between the sites. These terms vanish if $W_{ij} \cong 0$ (small overlap).

2.3 Flexible LPG

In this current work, we expand the LPG method to allow for the widths of the site Gaussians to change with time. For simplicity, we have assumed that width tensor $\tilde{\boldsymbol{M}}_i$ is diagonal. Now the Gaussian has the form:

$$\eta_i = |N_i| \exp[-\tfrac{1}{2}(\boldsymbol{x} - \bar{x}_i)\cdot\tilde{\boldsymbol{M}}_i\cdot(\boldsymbol{x} - \bar{x}_i) + i\bar{p}_i\cdot\boldsymbol{x}] \tag{22}$$

where the normalization constant is determined to be

$$|N_i| = \det\left(\frac{\mathrm{Re}\ \tilde{\boldsymbol{M}}_i}{\pi^N} \right)^{1/4} \tag{23}$$

$\tilde{\boldsymbol{M}}_i = \tilde{\boldsymbol{M}}_i(t)$ so that it is time dependent and complex. Notice the importance of using a complex width tensor. If $\tilde{\boldsymbol{M}}_i$ was only allowed to be real, use of the Frenkel variational method would result in canceling of all the propagating terms in $\tilde{\boldsymbol{M}}_i$. The Gaussian has a real normalization constant, since its phase factor is absorbed into the complex ψ_i.

The overlap is now slightly more complicated. Remembering the definition from eqn. (16) we find:

$$W_{ij} = \left(\frac{4\ \det(\mathrm{Re}\ \tilde{\boldsymbol{M}}_i^*)\cdot\det(\mathrm{Re}\ \tilde{\boldsymbol{M}}_j)}{\det(\tilde{\boldsymbol{M}}_i^* + \tilde{\boldsymbol{M}}_j)^2} \right)^{1/4} \exp\left\{ -\frac{1}{2} (\tilde{\boldsymbol{M}}_i^* + \tilde{\boldsymbol{M}}_j)^{-1} \times [(\bar{x}_i - \bar{x}_j)\cdot\tilde{\boldsymbol{M}}_i^*\cdot\tilde{\boldsymbol{M}}_j\cdot(\bar{x}_i - \bar{x}_j) + (\bar{p}_i - \bar{p}_j)^2 + 2i(\bar{p}_i - \bar{p}_j)\cdot(\tilde{\boldsymbol{M}}_i^*\cdot\bar{x}_i + \tilde{\boldsymbol{M}}_j\cdot\bar{x}_j)] \right\} \tag{24}$$

The new form of the Gaussian is now substituted into eqn. (14). Once again we use the Frenkel variational principle,

which leads here to:

$$A = \int_0^\infty \mathrm{d}t \Bigg\{ \sum_{j=1}^{\text{sites}} \Bigg[\Bigg(\bar{E}_j + \bar{\boldsymbol{x}}_j \cdot \boldsymbol{\Delta}_j - \frac{1}{4} \Bigg(\mathrm{Re}\, \tilde{\boldsymbol{M}}_j^{-1} \cdot \frac{\partial \mathrm{Im}\, \tilde{\boldsymbol{M}}_j}{\partial t} \Bigg) + \bar{\boldsymbol{x}}_j \cdot \frac{\partial \bar{\boldsymbol{p}}_j}{\partial t} \Bigg) |\psi_j|^2 - i\psi_j^* \frac{\partial \psi_j}{\partial t} \Bigg] + \sum_{j,k=1}^{\text{sites}} W_{jk} h_{jk} \psi_j^* \psi_k \Bigg\} \quad (25)$$

The functional A has the same form as for the frozen LPG, except for the dependence on $\tilde{\boldsymbol{M}}_i$.

Minimizing A with respect to ψ_i^* follows exactly as before to give:

$$\frac{\partial \psi_i}{\partial t} = -i \Bigg[\Bigg(\bar{E}_i + \bar{\boldsymbol{x}}_i \cdot \boldsymbol{\Delta}_i - \frac{1}{4} \mathrm{Tr} \Bigg(\mathrm{Re}\, \tilde{\boldsymbol{M}}^{-1} \cdot \frac{\partial \mathrm{Im}\, \tilde{\boldsymbol{M}}_i}{\partial t} \Bigg) + \bar{\boldsymbol{x}}_i \cdot \frac{\partial \bar{\boldsymbol{p}}_i}{\partial t} \Bigg) \psi_i + \sum_{j=1}^{\text{sites}} h_{ij} \psi_j W_{ij} \Bigg] \quad (26)$$

Minimizing A with respect to $\bar{\boldsymbol{x}}_i$ gives:

$$\frac{\partial \bar{\boldsymbol{p}}_i}{\partial t} = -\Bigg\{ \bar{\boldsymbol{x}}_i \cdot \kappa + \boldsymbol{\Delta}_i + 2\mathrm{Re} \Bigg[\frac{1}{\psi_i} \sum_{j=1}^{\text{sites}} h_{ij} \psi_j W_{ij} (\tilde{\boldsymbol{M}}_i^* + \tilde{\boldsymbol{M}}_j)^{-1} \times (\tilde{\boldsymbol{M}}_i^* \cdot \tilde{\boldsymbol{M}}_j \cdot (\bar{\boldsymbol{x}}_j - \bar{\boldsymbol{x}}_i) + i\tilde{\boldsymbol{M}}_i^* \cdot (\bar{\boldsymbol{p}}_j - \bar{\boldsymbol{p}}_i) \Bigg] \Bigg\} \quad (27)$$

A canonical transform is done for the derivation of the equation of motion for $\bar{\boldsymbol{x}}_i$. The resulting equation for the propagation of $\bar{\boldsymbol{x}}_i$ is:

$$\frac{\partial \bar{\boldsymbol{x}}_i}{\partial t} = \frac{\bar{\boldsymbol{p}}_i}{m} + 2\mathrm{Re} \Bigg[\frac{1}{\psi_i} \sum_{j=1}^{\text{sites}} h_{ij} \psi_j U_{ij} (\tilde{\boldsymbol{M}}_i^* + \tilde{\boldsymbol{M}}_j)^{-1} \cdot [(\bar{\boldsymbol{p}}_j - \bar{\boldsymbol{p}}_i) - i\tilde{\boldsymbol{M}}_j \cdot (\bar{\boldsymbol{x}}_j - \bar{\boldsymbol{x}}_i)] \Bigg] \quad (28)$$

where a transformed overlap is defined as:

$$U_{ij} = W_{ij} \mathrm{e}^{i(\bar{\boldsymbol{x}}_i \cdot \bar{\boldsymbol{p}}_i - \bar{\boldsymbol{x}}_j \cdot \bar{\boldsymbol{p}}_j)} \quad (29)$$

Now to find the equations of motion for the $\tilde{\boldsymbol{M}}_i$, first the derivative of A is taken with respect to Re $\tilde{\boldsymbol{M}}_i$. This gives:

$$\frac{\partial \mathrm{Im}\, \tilde{\boldsymbol{M}}_i}{\partial t} = -2[\mathrm{Re}\, \tilde{\boldsymbol{M}}_i]^2 \cdot \mathrm{Re} \Bigg\{ \frac{1}{\psi_i} \sum_{j=1}^{\text{sites}} h_{ij} \psi_j W_{ij} \times [\mathrm{Re}\, \tilde{\boldsymbol{M}}_i^{-1} - 2(\tilde{\boldsymbol{M}}_i^* + \tilde{\boldsymbol{M}}_j)^{-1} - 2[(\tilde{\boldsymbol{M}}_i^* + \tilde{\boldsymbol{M}}_j)^{-1} (\tilde{\boldsymbol{M}}_j (\bar{\boldsymbol{x}}_i - \bar{\boldsymbol{x}}_j) + i(\bar{\boldsymbol{p}}_i - \bar{\boldsymbol{p}}_j))^2]] \Bigg\} \quad (30)$$

Now a canonical transform is done, but this one interchanges Im $\tilde{\boldsymbol{M}}_i$ with Re $\tilde{\boldsymbol{M}}_i$. The transform is $\exp(-i\mathrm{Im}\, \tilde{\boldsymbol{M}}_i \cdot \mathrm{Re}\, \tilde{\boldsymbol{M}}_i^{-1})$. Applying this transform, it can be shown that:

$$\frac{\partial \mathrm{Re}\, \tilde{\boldsymbol{M}}_i}{\partial t} = -2[\mathrm{Re}\, \tilde{\boldsymbol{M}}_i]^2 \cdot \mathrm{Re} \Bigg\{ \frac{i}{\psi_i} \sum_{j=1}^{\text{sites}} h_{ij} \psi_j W_{ij} \times [\mathrm{Re}\, \tilde{\boldsymbol{M}}_i^{-1} - 2(\tilde{\boldsymbol{M}}_i^* + \tilde{\boldsymbol{M}}_j)^{-1} - 2[(\tilde{\boldsymbol{M}}_i^* + \tilde{\boldsymbol{M}}_j)^{-1} (\tilde{\boldsymbol{M}}_j (\bar{\boldsymbol{x}}_i - \bar{\boldsymbol{x}}_j) + i(\bar{\boldsymbol{p}}_i - \bar{\boldsymbol{p}}_j))]^2 \Bigg\} \mathrm{e}^{(-i/4)(\mathrm{Re}\, \tilde{\boldsymbol{M}}_i^{-1} \cdot \mathrm{Im}\, \tilde{\boldsymbol{M}}_i - \mathrm{Re}\, \tilde{\boldsymbol{M}}_j^{-1} \cdot \mathrm{Im}\, \tilde{\boldsymbol{M}}_j)} \quad (31)$$

For the flexible Gaussian, we now have extra complex degrees of freedom so that there are $2 + 4N$ equations to be solved.

We will compare the results of the above three methods (TDSCF, flexible LPG and frozen LPG) to a full calculation whereby one solves:

$$\frac{\partial \Psi(i, \bar{\boldsymbol{x}}, t)}{\partial t} = -i \Bigg\{ \Bigg(\frac{\boldsymbol{p}^2}{2m} + \frac{\boldsymbol{x} \cdot \kappa \cdot \boldsymbol{x}}{2} + \boldsymbol{x} \cdot \boldsymbol{\Delta}_i \Bigg) \Psi(i, \boldsymbol{x}, t) + \sum_{j=1}^{\text{sites}} h_{ij} \Psi(j, \boldsymbol{x}, t) \Bigg\} \quad (32)$$

3 Model application

3.1 Model system

For our test model, we study a two-site electron transfer coupled to a single harmonic oscillator. The 'system' is defined as the electronic part and the bath is defined as a single ($N = 1$) vibrational mode. Then the Hamiltonian with local mixing can be written as:

$$H = \begin{bmatrix} 1 & 0 \\ 0 & 1 \end{bmatrix} \frac{p^2}{2m} + \begin{bmatrix} m\omega_1^2 & 0 \\ 0 & m\omega_2^2 \end{bmatrix} \frac{x^2}{2} + \begin{bmatrix} \epsilon_1 & \Gamma \\ \Gamma & \epsilon_2 \end{bmatrix} + \begin{bmatrix} \Delta & \\ & -\Delta \end{bmatrix} x \quad (33)$$

where the matrix notation refers to the electronic sites. The TDSCF and LPG propagations were done with a Runge–Kutta method. The exact propagation was done with a Chebyshev approach.[35]

3.2 Results

We performed several studies which are detailed below. The studies demonstrate how both versions of the LPG equations are more accurate than TDSCF, especially when different frequencies are used for each well. The flexible Gaussians are not better for short times but significantly improve over the frozen in intermediate times.

The conditions for the simulations are shown in Table 1. The first four cases are similar to those studied in an earlier letter (where the frozen LPG method was discussed). In those cases, the oscillator mass was 17 u, the frequency $\omega = 0.05$ eV and the coupling small $\Delta = 0.03$ eV. The coupling was chosen to be small because in future simulations the LPG approximation will only be used for coordinates (x_n) with small mixing values Δ_{in}. The strongly mixed coordinates will be calculated exactly. In all cases, we placed the initial wavepacket on diabat 1, with zero momentum. The initial values of $\bar{x}_{1,2}$ are given in Table 1.

A practical difficulty is that the equations for the Gaussian position and width are undefined for sites that have zero population ($\psi_i = 0$). For that reason we always initially placed a small component on the initially-empty diabat. In our case we used $\psi_1 = (0.99)^{1/2}$ and the remaining portion, 0.1, on diabat 2. On both diabats, the Gaussians were initially given the same average position $\bar{x}_i$. In practice, we found that the results were insensitive to the value of the wavefunction coefficients on the second diabat, as long as these were sufficiently small.

We examined the probability that the electron is on the initial site, which we denote simply $|\Psi_1|^2$ (formally referring to $\int |\Psi(i = 1, x, t)|^2 \mathrm{d}x$). Both LPG methods are significantly better than TDSCF. For several vibrational periods, they follow the full calculation reasonably well, as shown in Fig. 2.

In the second case (Fig. 3), the two diabats no longer have the same minimum, but are offset by 0.01 eV. Again both LPG approximations closely follow the complete calculation, for about 230 fs; and again the flexible LPG does slightly better a little further out in time, but not as well initially.

Note that in the third case (Fig. 4), even when $|\Psi_1|^2$ oscillates in a very irregular fashion, both LPG methods follow the

Table 1 Parameters for the four test cases I–IV

Parameter	I	II	III	IV
ϵ_1/eV	2.00	2.01	2.01	2.00
ϵ_2/eV	2.00	2.00	2.00	2.00
Γ/eV	0.01	0.01	0.01	0.01
$\bar{x}_{1,2}$/Å	0.15	0.15	0.03	0.15
ω_1/eV	0.05	0.05	0.05	0.05
ω_2/eV	0.05	0.05	0.05	0.075

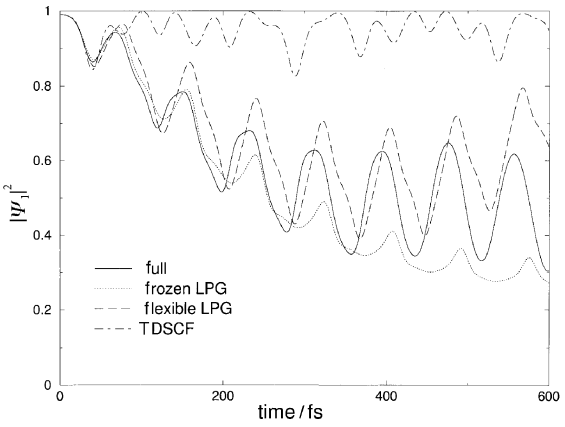

Fig. 2 Comparison of $|\Psi_1|^2$ as a function of time for the case that the diabats have equally deep potential minimum (case I) with the initial wavepacket placed far from the origin, $\bar{x}$ at 0.15 Å. Shown are the results of the exact, both LPGs and the TDSCF calculations.

full calculation quite well, especially in comparison with TDSCF.

In the rest of this section we examine the flexible *vs.* frozen Gaussians features. All our simulations refer henceforth to case I. First, we revisit Fig. 2, and note that though initially the flexible LPG performs somewhat less accurately than the

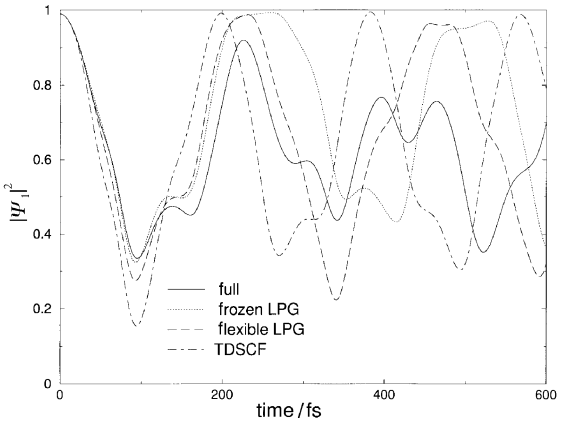

Fig. 3 Comparison of $|\Psi_1|^2$ as a function of time for case II. The energy of diabat 1 is displaced with respect to diabat 2 ($\epsilon_1 - \epsilon_2 = 0.01$ eV) and the initial wavepacket is placed far from the origin, $\bar{x}$ at 0.15 Å. Shown are the results of the exact, both LPGs and TDSCF calculations.

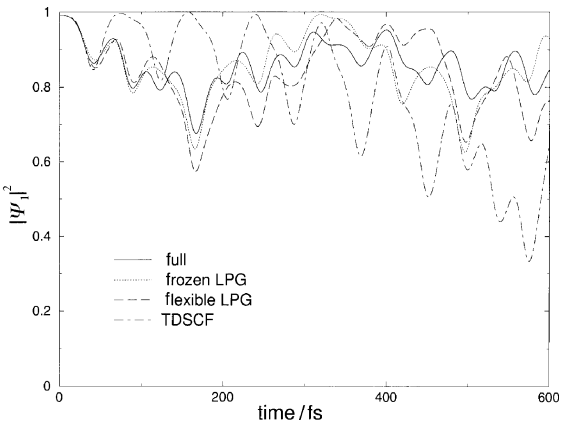

Fig. 4 Comparison of $|\Psi_1|^2$ as a function of time for case III. The energy of diabat 1 is displaced with respect to diabat 2 ($\epsilon_1 - \epsilon_2 = 0.01$ eV) and the initial wavepacket is now placed close to the origin, $\bar{x}$ at 0.03 Å. Shown are the results of the exact, both LPGs and the TDSCF calculations.

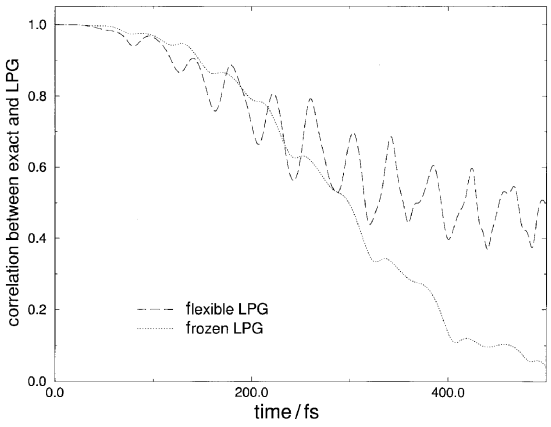

Fig. 5 The absolute value of the correlation between the exact time-dependent function and the LPG function, shown for both LPG methods (frozen and flexible). Case I is used.

frozen LPG, it does better at intermediate times, due to the extra degrees of freedom. To see this better, we plot in Fig. 5 the absolute value of the correlation between the exact and the approximate wavefunction (for case I), which shows again that initially that the frozen LPG does better over short times. The reason for the discrepancy is, heuristically, that the wavefunction on the second diabat is not truly a single Gaussian, but is more accurately described by a sum of Gaussians, one for each time that the Gaussian in the first diabat reaches the crossing point. Thus, it has components extended over different regions. The flexible Gaussian results can be somewhat skewed as the flexible Gaussian 'tries' to extend, so as to be similar to a multi-Gaussian wavefunction; the frozen Gaussian is not modified, and therefore performs better for short times. At long times, however, the added degrees of freedom of the flexible Gaussian make it superior.

To further elucidate the effect of allowing the width to vary in the flexible Gaussians, we looked at two extensions of case 1. In the original runs, we chose M to be one over the square of the natural width, which for all our cases is 200 Å^{-2}. In the extensions, we used two different initial values for M: $M = 100$ Å^{-2} (the Gaussian is the natural width $\times \sqrt{2}$) and $M = 400$ Å^{-2} (the Gaussian is $1\sqrt{2}$) of the natural width). The results for the LPGs are shown in Fig. 6. The results for frozen LPG [Fig. 6(a)] are very dependent on the initial width chosen. In comparison, the flexible LPG [Fig. 6(b)] is very robust. Thus, for large ranges of initial widths chosen, the flexible LPG gives very good results. For the cases we have chosen here (one-dimensional, two-site system), it is very simple to calculate the natural width; however, for multi-dimensions, anharmonicities will make the task of choosing a 'good' width more difficult. The flexible LPG will perform better in such cases.

For the three initial conditions for case I, we looked at the width with respect to time (Fig. 7). There are two competing processes occurring. At the boundaries of the potentials there is reflection of the wavepacket which narrows it (increase in M). Each upward spike in M in Fig. 7 corresponds to this reflection. The other effect is the broadening that occurs as the amplitude of the wavepacket 'hops' from one site to the other, each time the wavepacket passes the location of the curve crossing. It is clear that at intermediate times this broadening is dominant and is probably the reason that the flexible LPG performs well at intermediate times.

For a one-dimensional case, there seems to be only moderate improvement between the frozen and flexible LPG, until long times are used. We believe this is for the following reasons. Under the conditions chosen, the frozen LPG already does remarkably well because the potentials are only slightly anharmonic; therefore, the extra degrees of freedom ($\tilde{M}_i$) are

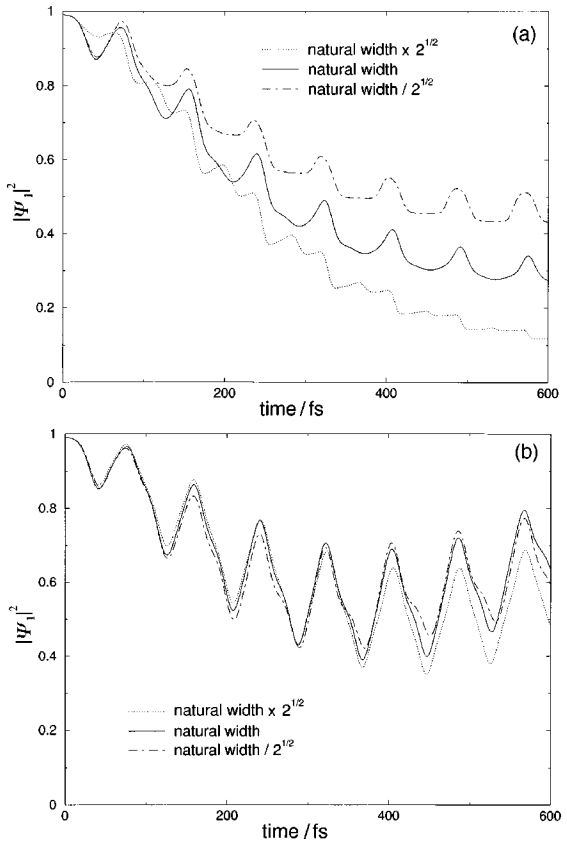

Fig. 6 Comparison of $|\Psi_1|^2$ as a function of time for case I, with three different initial values for M_i: 100, 200 and 400 Å^{-2}; (a) shows the frozen LPG, (b) shows the flexible LPG.

only nominally able to improve the propagation of the wavefunction. We do expect to see an improvement in the case of multi-dimensions. In this case, the flexible LPG method will allow coupling between the dimensions (*i.e.*, spreading in one dimension while shrinking in another, as well as rotating the coordinates). This should lead to a significant improvement over the frozen LPG.

Finally, we note that the cases presented above have all been presented for a very specific Hamiltonian, where the frequencies on each well are identical. In a preliminary investigation (Fig. 8), we examined the performance of the LPG on a physically important case where the frequencies are also site-dependent. Specifically, we used case I above, but modified the frequency on the second adiabat by 50% to be 0.075. In that case the LPGs were significantly better than TDSCF; they

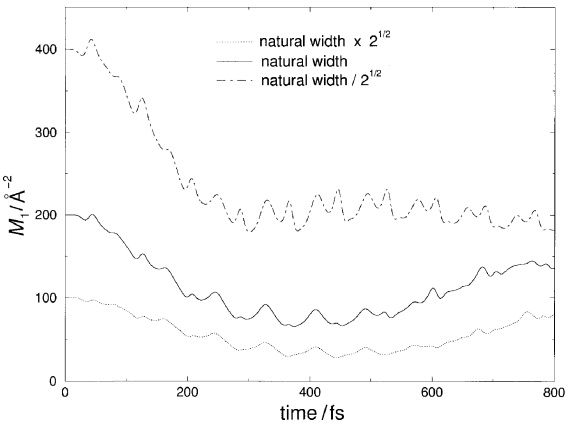

Fig. 7 Comparison of M_1 with respect to time for three different initial values: 100, 200 and 400 Å^{-2}.

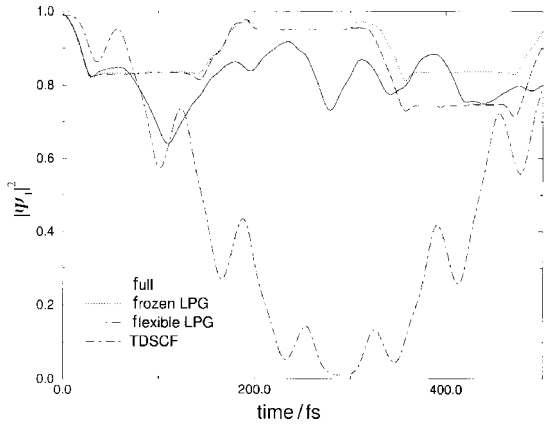

Fig. 8 Similar to Fig. 2, except that now the frequencies on each diabat are modified: on the first diabat the frequency is left at 0.05 eV, while on the second diabat it is modified to be 0.075 eV.

deviated by ~10–15% from the exact result while the TDSCF varied by up to ~80%. This is very encouraging for future extensions, since many physical systems have bath-frequencies which are strongly dependent on the system site.

4 Future extensions

Because of its speed and ability to handle weakly coupled systems, LPG is naturally appropriate for calculating the quantum dynamics of large systems. We have done some initial work on a problem of proton (rather than electron) transfer coupled to a simple bath, *i.e.*, a heavier atom motion, which is treated with LPG. In that problem, the quasi-continuous proton degree of freedom is represented by multiple sites (one 'site' for each degree of freedom) while the other degree of freedom is treated with LPG. Initial results have shown the frozen and flexible LPG to perform significantly better than TDSCF. We will present these results in future work.

5 Conclusions

We have presented a method, LPG, that accurately mimics a fully quantum propagation for several vibrational periods for weakly coupled systems without requiring extensive computational effort. The method assumes that the bath wavefunction at each site is (and remains) a Gaussian, but unlike the mean-field approximation, the Gaussian parameters depend explicitly on the system state ('site'). We tested two forms of the LPGs, one is the frozen Gaussian in which the width is kept constant, the second is the flexible Gaussian in which the width is complex and propagates in time. Both the flexible and frozen LPG methods performed better than the TDSCF calculations. In the simple one-dimensional case presented here, there is only a slight improvement with the flexible LPG. However, flexible Gaussians could be important in multi-dimensional problems, since they allow for modified coupling between bath degrees of freedom, which changes with system states. Specifically, non-diagonal width tensors which change with system sites could be used to represent the change of the normal mode character of the bath upon the change of system state (*e.g.*, when the system changes from reactants to products).

Either of the LPG methods can be used in much larger simulations than the ones presented here. The strongly coupled system modes will be done with an explicit grid-type calculation, and the bath can be accurately treated with LPG. This will extend the types of problems with correlations that can be done quantum mechanically, including many-body

chemical reactions and electron transfer on surfaces or in large molecules. As mentioned earlier, we have already extended the frozen LPG to a system with a large number of sites and will be presenting our results soon.

6 Acknowledgements

We are grateful to Jeffrey Zink and Uri Peksin for useful discussions, and to a referee of this paper for useful comments and pointing out appropriate references. This work was supported by NSF grant CHE97-27084 and by the Alfred P. Sloan Fellowship (D.N.). Partial support from KOSEF is acknowledged (T.J.P.).

7 References

1 D. Neuhauser, *J. Chem. Phys.*, 1994, **100**, 9272.
2 D. C. Clary, *J. Phys. Chem.*, 1994, **98**, 10678.
3 W. Zhu, J. Z. H. Zhang and D. H. Zhang, *Chem. Phys. Lett.*, 1998, **292**, 46.
4 M. F. Herman and E. Kluk, *Chem. Phys.*, 1984, **91**, 27.
5 K. G. Kay, *J. Chem. Phys.*, 1994, **101**, 2250.
6 S. Garashchuk, F. Grossman and D. Tannor, *J. Chem. Soc., Faraday Trans.*, 1997, **93**, 781.
7 A. E. Cardenas and R. D. Coalson, *Chem. Phys. Lett.*, 1997, **265**, 71.
8 M. L. Brewer, J. S. Hulme and D. E. Manolopoulus, *J. Chem. Phys.*, 1997, **106**, 4832.
9 E. R. Bittner, B. J. Schwartz and P. J. Rossky, *J. Mol. Struct.*, 1997, **389**, 203.
10 C. C. Martens and J. Y. Fang, *J. Chem. Phys.*, 1997, **106**, 4918.
11 M. Ovchinnikov and V. A. Apkarian, *J. Chem. Phys.*, 1998, **108**, 2277.
12 V. S. Batista and W. H. Miller, *J. Chem. Phys.*, 1998, **108**, 498.
13 D. Antoniou and S. D. Schwartz, *J. Chem. Phys.*, 1998, **108**, 3620.
14 R. Egger and C. H. Mak, *Phys. Rev. B*, 1994, **50**, 15210.
15 M. Topaler and N. Makri, *J. Chem. Phys.*, 1994, **101**, 7500.
16 F. Matzkies and U. Manthe, *J. Chem. Phys.*, 1997, **106**, 2646.
17 A. D. Hammerich, R. Kosloff and M. A. Ratner, *Chem. Phys. Lett.*, 1990, **171**, 97.
18 R. Baer and R. Kosloff, *J. Chem. Phys.*, 1997, **106**, 8862.
19 P. Jungwirth, E. Fredji and R. B. Gerber, *J. Chem. Phys.*, 1997, **107**, 8963.
20 R. B. Gerber, V. Buch and M. A. Ratner, *Chem. Phys. Lett.*, 1982, **91**, 173.
21 E. J. Heller, *J. Chem. Phys.*, 1975, **62**, 1544.
22 E. J. Heller, *J. Chem. Phys.*, 1976, **65**, 4979.
23 E. J. Heller, *J. Chem. Phys.*, 1981, **75**, 2923.
24 M. J. Davis and E. J. Heller, *J. Chem. Phys.*, 1979, **71**, 3383.
25 A. Diz, E. Deumens and Y. Ohrn, *Chem. Phys. Lett.*, 1990, **166**, 203.
26 M. Ben-Nun and R. D. Levine, *Chem. Phys.*, 1995, **201**, 163.
27 N. P. Blake and H. Metiu, *J. Chem. Phys.*, 1995, **103**, 4455.
28 N. Markovic and G. D. Billing, *Chem. Phys.*, 1997, **224**, 53.
29 M. Ben-Nun and T. J. Martinez, *J. Chem. Phys.*, 1998, **108**, 7244.
30 M. Ben-Nun and T. J. Martinez, *J. Chem. Phys.*, 1998, **109**.
31 R. Silbey and R. A. Harris, *J. Phys. Chem.*, 1989, **93**, 7062.
32 B. Jackson, *J. Chem. Phys.*, 1989, **90**, 1458.
33 J. Frenkel, *Wave Mechanics*, Clarendon, Oxford, 1934.
34 S. M. Anderson, J. I. Zink and D. Neuhauser, *Chem. Phys. Lett.*, 1998, **291**, 387.
35 R. Kosloff, *J. Chem. Phys.*, 1988, **92**, 2087.

Paper 8/08989B